Degenerate four-wave mixing of optical vortices assisted by self-phase and cross-phase modulation

G. Maleshkov[1], P. Hansinger[2], I. L. Garanovich[3], D. Skryabin[4], D. N. Neshev[3], A. Dreischuh[1], G. G. Paulus[2]

[1]Department of Quantum Electronics, Faculty of Physics, Sofia University, Sofia, Bulgaria
[2]Institute of Optics and Quantum Electronics, Faculty of Physics and Astronomy, Friedrich-Schiller-University, Jena, Germany
[3]Nonlinear Physics Center, Research School of Physics and Engineering, Australian National University, Canberra, Australia
[4]Centre for Photonics and Photonic Materials, Department of Physics, University of Bath, Bath, United Kingdom

ABSTRACT

We study theoretically the non-phase-matched degenerate four-wave mixing of type $\omega_s = 2\omega_1 - \omega_2$, involving beams carrying two-dimensional spatial phase dislocations in the form of singly-charged optical vortices (OVs). Accompanying third-order nonlinear processes in the non-resonant nonlinear medium (NLM), which are accounted for, are self- and cross-phase modulation. In the case of pump OV beams with identical topological charges the model predicts the generation of signal beams carrying OVs of the same charge. If the pump beams carry OVs with opposite charges, the generated signals are predicted to carry triply charged vortices which, in the case of a non-negligible initial free-space propagation from the plane of vortex generation to the NLM, decay inside the NLM into three singly-charged vortices with highly overlapping cores.

Keyword list: four-wave mixing, Kerr nonlinearity, self-focusing, optical vortex, phase dislocation, phase matching

1. INTRODUCTION

Degenerate four-wave mixing (DFWM) is a third-order nonlinear process in which two waves (*i* and *j*) interact in a nonlinear medium to produce an output at sum and/or difference frequencies[1] $\omega_s = 2\omega_i \pm \omega_j$. Four-wave mixing is related to self-phase modulation (SPM) and cross-phase modulation (XPM) since all these effects originate from the same (Kerr) nonlinearity and differ only in terms of degeneracy of the waves involved. XPM can be expressed as $\omega_s = \omega_s + \omega_j - \omega_j$, whereas the relation for SPM is $\omega_s = \omega_s + \omega_s - \omega_s$. Importantly, neither SPM nor XPM generate new distinct frequencies. Rather both, self- and cross-phase modulation, change the medium's refractive index in a nonlinear way thus giving rise to nonlinear phase shifts and to spectral broadening of the already existing frequency components.

Optical vortices (OVs) are associated with the presence of a spiral phase dislocation in the wavefront of a light beam that determines its phase and intensity structure. The study of OVs has received special attention in recent years due to a variety of potential applications including particle micro-manipulation[2], imaging[3], interferometry[4], quantum information[5], high-resolution microscopy, lithography[6] etc. In experiments conducted with Rb[7] and cold Cs atoms[8] it is demonstrated that the optical angular momentum carried by an OV beam can be transferred, through interaction with the atomic system by means of a FWM process, to another light beam mode. Clearly, OVs at various wavelengths or even multi-color OVs are desirable for such applications. The transformation of the topological structure of an OV beam under multiwave mixing in the media with resonant nonlinearity has been analyzed theoretically[9]. In a second-harmonic generation process the OV topological charge and orbital angular momentum per photon becomes doubled[10,11]. Multi-colored OVs can be created through nonlinear frequency conversion processes (FWM), e.g. via optical phase conjugation[12]. Unlike OV propagation in a Raman[13] or quadratic nonlinear medium[14], the FWM process is expected to preserve the topological charge of the OVs and can be an important factor for white-light vortex generation. However, as the FWM process may be accompanied by

noticeable self- and induced focusing (spatial analogs of SPM and XPM, respectively), special attention should be paid to the vortex integrity. The OV dynamics in a nonlinear medium is known to lead to vortex break-up or disintegration[15-17]. Recently we reported[18] the first experimental demonstration of femtosecond supercontinuum generation by an optical vortex beam. The results demonstrate that the initial spatial profile of the optical vortex is well preserved in the process of supercontinuum generation. However, the generated continuum did not carry the phase structure of the initial beam and appeared as a wide white-light background surrounding the fundamental OV. We have found that strong diffraction of the supercontinuum generated from each individual filament formed on the bright vortex ring is the reason for the observed white-light background.

Here we expand our earlier studies and analyze numerically the process of FWM with singular beams. Our studies show that the coherent generation of new frequency components in the FWM process provides a viable path for generation of white-light singular beams despite the azimuthal instabilities of the optical vortices in Kerr-type nonlinear media.

2. THEORETICAL MODEL AND NUMERICAL PROCEDURE

The model we use in this work is based on a set of four nonlinear partial differential equations (1) describing the evolution of the four slowly-varying amplitudes A_m of four distinct spectral components at frequencies ω-δ, ω, ω+δ, and ω+2δ

$$i\frac{\partial A_m}{\partial z} + L_{Diff}^{\omega} k_m A_m + \frac{\lambda_m n(\lambda_\omega)}{2\lambda_\omega n(\lambda_m)} \Delta_\perp A_m + \gamma\left\{ \left|A_m\right|^2 A_m + 2\sum_{n\neq m} \left|A_n\right|^2 A_m + H_m \right\} = 0 \quad , \tag{1}$$

($m, n = \omega-\delta, \omega, \omega+\delta, \omega+2\delta$). Here the terms in the brackets account for the self-phase modulation (SPM), for the cross-phase modulation (XPM), and

$$H_{\omega-\delta} = 2A_{\omega+2\delta}^{*} A_\omega A_{\omega+\delta} \exp(i\Delta k_1 z L_{Diff}^{\omega}) + A_\omega^2 A_{\omega+\delta}^{*} \exp(i\Delta k_2 z L_{Diff}^{\omega}) \quad , \tag{2a}$$

$$H_{\omega} = 2A_{\omega}^{*} A_{\omega+\delta} A_{\omega-\delta} \exp(i\Delta k_3 z L_{Diff}^{\omega}) + 2A_{\omega+\delta}^{*} A_{\omega+2\delta} A_{\omega-\delta} \exp(i\Delta k_4 z L_{Diff}^{\omega}) + A_{\omega+\delta}^2 A_{\omega+2\delta}^{*} \exp(i\Delta k_5 z L_{Diff}^{\omega}) , \tag{2b}$$

$$H_{\omega+\delta} = 2A_{\omega} A_{\omega+2\delta} A_{\omega-\delta} \exp(i\Delta k_6 z L_{Diff}^{\omega}) + 2A_{\omega+\delta}^{*} A_{\omega+2\delta} A_{\omega} \exp(i\Delta k_7 z L_{Diff}^{\omega}) + A_\omega^2 A_{\omega-\delta}^{*} \exp(i\Delta k_8 z L_{Diff}^{\omega}) , \tag{2c}$$

$$H_{\omega+2\delta} = 2A_{\omega-\delta}^{*} A_\omega A_{\omega+\delta} \exp(i\Delta k_9 z L_{Diff}^{\omega}) + A_{\omega+\delta}^2 A_\omega^{*} \exp(i\Delta k_{10} z L_{Diff}^{\omega}) \quad , \tag{2d}$$

reflect the different possible degenerate four-wave frequency mixing (FWM) processes, which depend on the respective phase matching relations

$$\begin{aligned}
\Delta k_1 &= k_\omega + k_{\omega+\delta} - 2k_{\omega+2\delta} - k_{\omega-\delta} & \qquad \Delta k_6 &= k_{\omega+2\delta} + k_{\omega-\delta} - k_\omega - k_{\omega+\delta} \\
\Delta k_2 &= 2k_\omega - k_{\omega+\delta} - k_{\omega-\delta} & \qquad \Delta k_7 &= k_{\omega+2\delta} + k_\omega - 2k_{\omega+\delta} \\
\Delta k_3 &= k_{\omega+\delta} + k_{\omega-\delta} - 2k_\omega & \qquad \Delta k_8 &= 2k_\omega - k_{\omega-\delta} - k_{\omega+\delta} \\
\Delta k_4 &= k_{\omega+2\delta} + k_{\omega-\delta} - k_{\omega+\delta} - k_\omega & \qquad \Delta k_9 &= k_\omega + k_{\omega+\delta} - k_{\omega-\delta} - k_{\omega+2\delta} \\
\Delta k_5 &= 2k_{\omega+\delta} - k_{\omega+2\delta} - k_\omega & \qquad \Delta k_{10} &= 2k_{\omega+\delta} - k_\omega - k_{\omega+2\delta}
\end{aligned} \quad . \tag{3}$$

k_m stands for the wavenumber of the m-th wave inside the NLM. Since we assume that initially the two high-intensity pump waves are at frequencies ω and ω+δ, it is natural to express the propagation coordinate z in units of diffraction lengths of one of these waves. We choose normalization to the Rayleigh diffraction length of the optical vortex nested in a wave of frequency ω, i.e. to $L_{Diff}^{\omega} = k_\omega a^2$, where a is the radius of the OV beam, being the same for both pump waves. The linear term in Eq.(1) comprising $\Delta_\perp$ accounts for the two-dimensional beam diffraction, whereas γ is the Kerr nonlinear coefficient.

Accounting for FWM, we solved the model system of differential equations (1) by means of a modified split-step Fourier method with a computational window spanning over 1024x1024 grid points for each wave. As a standard test we modeled the formation of a fundamental OV soliton by setting the sign of the nonlinearity γ to be

negative (for calibration purposes only). Unless stated otherwise, the intensities of the pump beams at frequencies $\omega+\delta$ and ω are kept equal to that needed to form a fundamental OV soliton in self-defocusing NLM when only SPM is accounted for and all FWM terms are neglected. *sign*(γ) is kept positive, which corresponds to CaF_2 as a suitable NLM. The two pump waves are chosen to have central wavelengths of 780 nm and 800 nm, i.e. the newly generated components will be centered at 761 nm and 821 nm. All necessary refractive indices and wave numbers are calculated at these wavelengths. Other waves at frequencies lower than ω-δ or higher than $\omega+2\delta$ are neglected in this model. Since CaF_2 is an isotropic material with a cubic crystal structure with inverse symmetry, collinear phase matching for the degenerate FWM processes $\omega_{s1}=2\omega_1-\omega_2$ and $\omega_{s2}=2\omega_2-\omega_1$ is not possible for the chosen pump wavelengths. Vector phase matching is however possible and requires angular offset between the pump beams of 3.9 mrad for signal wave at 761 nm and 2.7 mrad for that at 821 nm. Therefore, the collinear interaction geometry modeled numerically is to be classified as non-phase matched.

The input pump OV beams are described by

$$A = A_0 B(r)\tanh(r/r_0)\exp(im\varphi) \quad , \tag{4}$$

where A_0 is the peak field amplitude, $B(r)$ is the Gaussian bright background carrying the optical vortex $\left(B(r)=\exp\left\{-(r^2/r_{BG}^2)\right\}\right)$, $\tanh(r/r_0)$ describes the OV profile, and the integer m is the OV topological charge (m=±1 throughout this work). The background beam width r_{BG} was chosen sufficiently broader than the vortex core.

3. RESULTS

3.1. FWM of vortices with equal unit topological charges

The obtained numerical results for this case are summarized in Fig. 1. Some 8% of the total computational area is shown in each frame. The expected[9,12] transformations of the topological charges m of the pump OVs during the DFWM processes $\omega_{s1}=2\omega_1-\omega_2$ and $\omega_{s2}=2\omega_2-\omega_1$ are that $m_{s1}=2\times1-1=1$ and $m_{s2}=2\times1-1=1$. This means that both newly generated signal beams should contain vortices carrying equal unit TCs. This is clearly seen in the upper and lower frames in the last column of Fig. 1. Although the initial phase profile of both pump OV beams were chosen to be identical in this simulation (see phase profiles at $z_L=0$), after a free-space propagation up to $z_L=3L_{Diff}^{\omega}$ they accumulate phase difference due to their different (central) wavelengths. The difference between the diffraction spreading of the OV cores of the pump beams is too small to be seen in this mode of presentation but is noticeable when the cross-sections of the pump OVs are compared. The positive nonlinearity naturally contributes to the accelerated pump OV core broadening along the NLM (see the intensity profiles at $z_{NL}=0.5L_{Diff}^{\omega}$ in Fig. 1). However this is not the main reason for the newly generated dark beams to be so much broader. Rather, this is due to the fact that the FWM processes are intensity-dependent and the maximum pump beam intensity is along the vortex ring, which is much larger than the pump OV core. Comparing closely the 2D intensity profiles of the generated signal OVs one can see that the vortex ring of the signal component at the lower frequency ω-δ is somewhat modulated in azimuthal direction with a maximum (at this particular distance) on the right-hand side and with a minimum on the left-hand side. The detailed numerical analysis showed that this is due to the phase mismatch of the components involved in the DFWM process, which is stronger pronounced for the low-frequency signal than for the high-frequency signal. The energy density and phase profiles of the newly generated low-frequency wave *s1* at different nonlinear propagation distances shown in Fig. 2 support this statement. The maximum conversion efficiency of the process is 10^{-4}, which is a reasonable value considering there is no phase matching. As expected, we observed oscillations in the conversion efficiency vs. nonlinear propagation path length due to the energy flow from the pump waves to the signals and backwards. This is not seen on Fig. 2 since we normalized the energy density for each frame in order to underline the changes in the symmetry of the generated waves.

3.2. FWM of vortices with opposite topological charges

Let us assume that an azimuthal increase of the phase around the point phase dislocation of the OV in counter-clockwise direction refers to a TC m_j=+1. We will denote such a vortex as negatively-charged. The transformations of the topological charges of the pump OVs during the DFWM processes $\omega_{s1}=2\omega_1-\omega_2$ and $\omega_{s2}=2\omega_2-\omega_1$ are then $m_{s1}=2\times1-(-1)=3$ and $m_{s2}=2\times(-1)-1=-3$. Therefore, both newly generated signal beams should be triply charged optical vortices carrying opposite TCs. This is clearly seen in the respective phase profiles of the signal

beams shown in the upper and lower frames in Fig. 3 (right column). Since OVs with TCs higher than 1 are unstable against perturbations and the presence of a second signal wave the triply charged vortices decay into singly-charged ones. This is also well seen in the phase profiles of the signal beams shown in Fig. 3: Although the cores of the decaying vortices are still strongly overlapping, the three screw point dislocations separate as the distance increases. In addition, the vortex ring of the generated signal is more noticeably reshaped in the *s1*-wave. This appears to be due to the larger signal wavelength, which is diffracting stronger than the signal *s2* at the shorter wavelength.

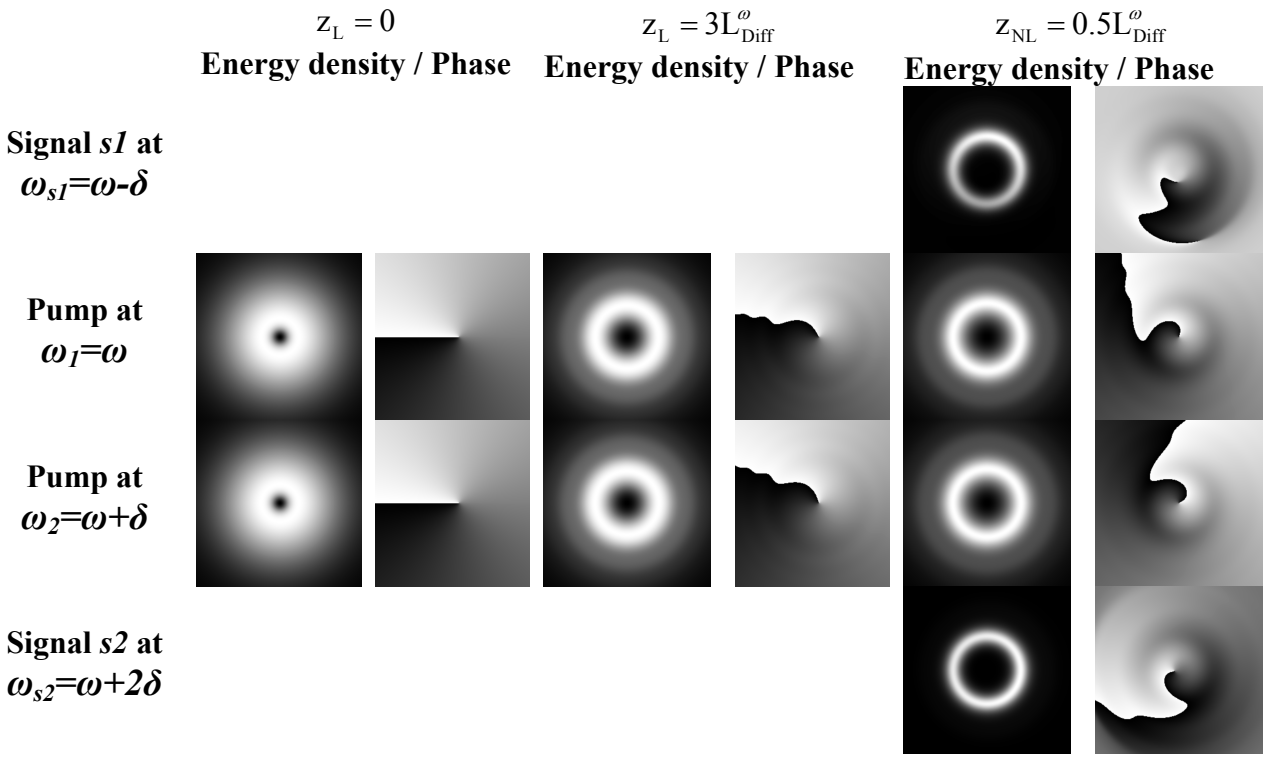

Fig. 1. Pump beams with equal TCs. Energy density (odd rows) and phase profiles (even rows) of the pump waves at frequencies ω and $\omega+\delta$ and of the newly generated waves at frequencies $\omega-\delta$ and $\omega+2\delta$ in the plane of OV beam generation (left two columns), after a free-space propagation distance $z_L = 3L_{Diff}^{\omega}$ (middle) and at the exit of the NLM after nonlinear propagation path length $z_{NL} = 0.5L_{Diff}^{\omega}$ (right two columns).

3.3. Pumping with an OV and a Gaussian beam

Another possible situation deserving attention is to have DFWM in which one singly-charged OV beam and a fundamental Gaussian beam with zero topological charge are involved. The results of this situation are summarized in Fig. 4. In this case one should expect that one of the generated signals will carry a TC equal to +2 (according to the adopted convention for the TCs) and, the other one – an OV with a TC equal to -1. This can be clearly seen in the phase profiles of the signal beams shown in the right column in Fig. 4. As a result of SPM, XPM and FWM the Gaussian pump beam becomes modulated in both amplitude and phase but does not acquire any topological charge. Under the perfect initial conditions of this numerical simulation the generated twofold-charged OV beam is predicted to be stable.

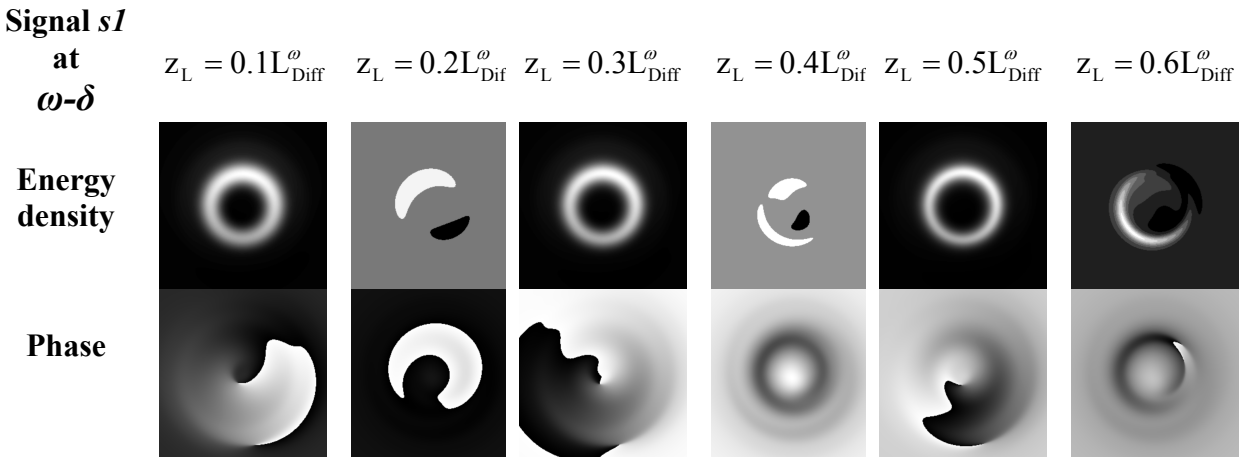

Fig. 2. Equal TCs of the pump beams. Energy density (upper row) and phase profiles (lower rows) of the low-frequency wave *s1* at different nonlinear propagation distances.

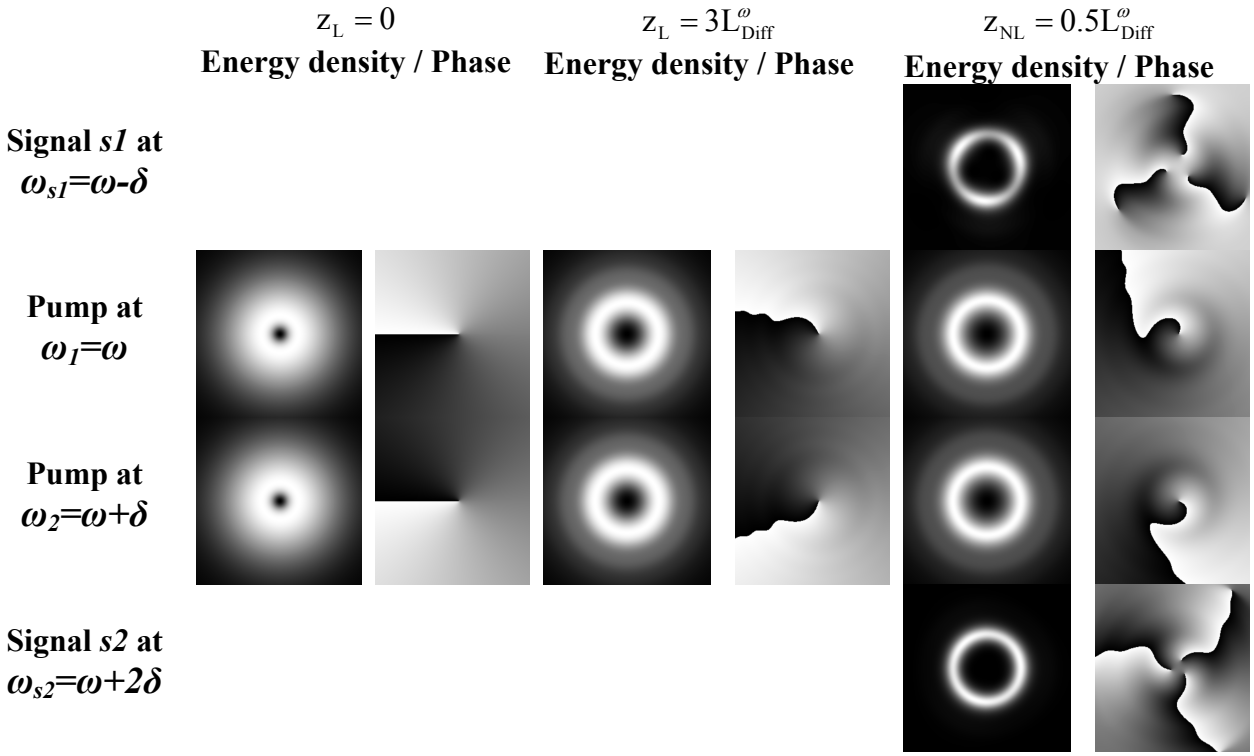

Fig. 3. Opposite TCs of the pump beams. Energy density (odd rows) and phase profiles (even rows) of the pump waves at frequencies ω and $\omega+\delta$ and of the newly generated waves at frequencies $\omega-\delta$ and $\omega+2\delta$ in the plane of OV beam generation (left two columns), after a free-space propagation distance $z_L = 3L_{Diff}^{\omega}$ (middle) and at the exit of the NLM after nonlinear propagation path length $z_{NL} = 0.5L_{Diff}^{\omega}$ (right two columns).

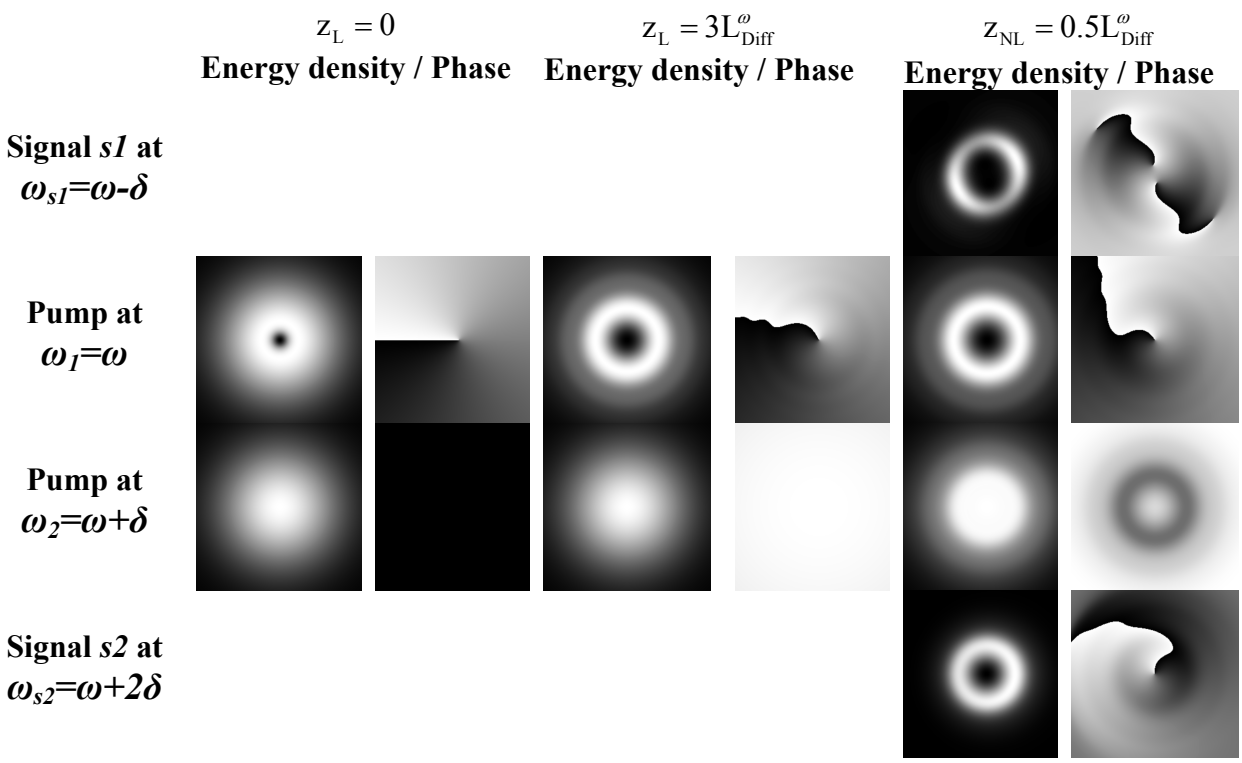

Fig. 4. Pump – OV and Gaussian beams. Energy density (odd rows) and phase profiles (even rows) of the OV and Gaussian pump waves at frequencies ω and $\omega+\delta$, respectively, and of the newly generated OVs at frequencies $\omega-\delta$ and $\omega+2\delta$ at the entrance of the NLM (left two columns), after nonlinear propagation path length $z_{NL} = 0.5L_{Diff}^{\omega}$ (middle) and at the exit of the NLM ($z_{NL} = 0.5L_{Diff}^{\omega}$; right two columns).

4. CONCLUSION

The reported numerical results on the non-phase-matched degenerate four-wave frequency mixing of the type $\omega_s = 2\omega_1 - \omega_2$ involving optical vortices confirm the transformation of the vortex topological charges of the newly-generated signal waves expected in such nonlinear process. The accompanying third-order nonlinear processes of self- and cross-phase modulation seem to noticeably influence the phase-mismatch, the amplitudes of the pump beams and the stability of the eventually generated multiply charged OVs. In the case of pump OV beams with identical topological charges we predict generation of signal beams carrying OVs with the same charges. When the pump beams carry OVs with opposite charges, the generated signals are expected to carry triply charged vortices which, however, will decay eventually and reshape the vortex rings of the signals. When one input pump beams is an OV and the other a fundamental Gaussian beam, generation of OVs with charge one and two and with opposite sign is predicted.

5. ACKNOWLEDGEMENT

The authors thank Yu. S. Kivshar and A. A. Sukhorukov for the useful discussions. We gratefully acknowledge funding by the National Science Fund (NSF) – Bulgaria (projects DO-02-0114/2008 and DRNF-02-8/2009), the Science Fund of the Sofia University (project 080/2010), the Australian Research Council, and the DFG in the framework of Forschergruppe 532 "Nichtlineare raum-zeitliche Dynamik in dissipativen und diskreten optischen Systemen".

6. REFERENCES

[1] Nienhuys, H.-K., Planken, P. C. M., van Santen, R. A. and Bakker, H. J., "Generation of mid-infrared pulses by $\chi^{(3)}$ difference frequency generation in CaF_2 and BaF_2," Opt. Lett. 26, 1350-1352 (2001).

[2] Grier, D. G., "A revolution in optical manipulation," Nature **424**, 810–816 (2003).

[3] Foo, G., xPalacios, D. G. and Swartzlander, Jr., G. A., "Optical vortex coronagraph," Opt. Lett. **30**, 3308–3310 (2005).

[4] Furhapter, S., Jesacher, A., Bernet, S. and Ritsch Marte, M., "Spiral interferometry," Opt. Lett. **30**, 1953–1955 (2005).

[5] Molina Terriza, G., Torres, J. P., and Torner, L., "Twisted photons," Nature Physics **3**, 305–310 (2007).

[6] Scott, T. F., Kowalski, B. A., Sullivan, A. C., Bowman, C. N. and McLeod, R. R. "Two-color single-photon photoinitiation and photoinhibition for subdiffraction photolithography," Science **324**, 913 (2009).

[7] Jiang, W., Chen, Q., Zhang, Y. and Guo, G.-C., "Computation of topological charges of optical vortices via nondegenerate four-wave mixing," Phys. Rev. A **74**, art. 043811 (2006).

[8] Barreiro, S., Tabosa, J. W. R., Torres, J. P., Deyanova, Y. and Torner, L., "Four-wave mixing of light beams with engineered orbital angular momentum in cold cesium atoms," Opt. Lett. **29**, 1515-1517 (2004).

[9] Romanov, O. G. and Tolstik, A. L. "Multiwave Mixing of Singular Light Beams in Resonant Media," Optics and Spectroscopy **105**, 753–757 (2008); "Wave front transformation of optical vortices with multiwave interactions in resonant media," J. Appl. Spectrosc. **76**, 370-376 (2009).

[10] Courtial, J., Dholakia, K., Allen, L. and Padgett, M. J., "Second-harmonic generation and the conservation of orbital angular momentum with high-order Laguerre-Gaussian modes," Phys. Rev. A **56**, 4193-4196 (1997).

[11] Dreischuh, A., Neshev, D. N., Kolev, V. Z., Saltiel, S., Samoc, M., Krolikowski, W., and Kivshar, Yu. S., "Nonlinear dynamics of two-color optical vortices in lithium niobate crystals," Optics Express **16**, 5406-5420 (2008).

[12] Lopez-Mariscal, C., Gutierrez-Vega, J. C., McGloin, D. and Dholakia, K. "Direct detection of optical phase conjugation in a colloidal medium," Optics Express **15**, 6330-6335 (2007).

[13] Gorbach, A. V. and Skryabin, D. V.,"Cascaded generation of multiply charged optical vortices and spatiotemporal helical beams in a Raman medium," Phys. Rev. Lett. **98**, art. 243601 (2007).

[14] Berzanskis, A., Matijosius, A., Piskarskas, A., Smilgevicius, V., Stabinis, A., "Conversion of topological charge of optical vortices in a parametric frequency converter," Opt. Commun. **140**, 273–276 (1997).

[15] Firth, W. J. and Skryabin, D. V., "Optical solitons carrying orbital angular momentum," Phys. Rev. Lett. **79**, 2450–2453 (1997).

[16] Tikhonenko, V., Christou, J. and Luther-Daves, B., "Spiraling bright spatial solitons formed by the breakup of an optical vortex in a saturable self-focusing medium," J. Opt. Soc. Am. B **12**, 2046–2052 (1995).

[17] Vuong, L. T., Grow, T. D., Ishaaya, A., Gaeta, A. L.,'t Hooft, G. W., Eliel, E. R. and Fibich, G., "Collapse of optical vortices," Phys. Rev. Lett. **96**, art. 13390 (2006).

[18] Neshev, D. N., Dreischuh, A., Maleshkov, G., Samoc, M. and Kivshar, Yu. S., "Supercontinuum generation with optical vortices," Optics Express, **18**, 18368-18373 (2010).